

# $X(3872)$ as a molecular $DD^*$ state in a potential model

Ian Woo Lee\*, Amand Faessler, Thomas Gutsche, Valery E. Lyubovitskij†

*Institut für Theoretische Physik, Universität Tübingen,  
Kepler Center for Astro and Particle Physics,  
Auf der Morgenstelle 14, D-72076 Tübingen, Germany*

(Dated: February 4, 2022)

We discuss the possibility that the  $X(3872)$  can be a hadronic  $DD^*$  bound state in the framework of a potential model. The potential is generated by the exchange of pseudoscalar, scalar and vector mesons resulting from the Lagrangian of heavy hadron chiral perturbation theory. The hadronic bound state configuration contains charged and neutral  $DD^*$  components, while orbital  $S$ - and  $D$ -waves are included. Isospin symmetry breaking effects are fully taken into account. We show that binding in the  $DD^*$  system with  $J^{PC} = 1^{++}$  already exists for a reasonable value of the meson-exchange regularization parameter of  $\Lambda \sim 1.2$  GeV. We also explore the possibility of hadronic  $BB^*$  bound states and show that binding can be achieved in the isoscalar limit for  $J^{PC} = 1^{++}$  or  $1^{+-}$ .

PACS numbers: 12.39.Fe, 12.39.Pn, 14.40.Gx, 36.10.Gv

Keywords: charm mesons, hadronic molecule, chiral Lagrangian, isospin symmetry violation

## I. INTRODUCTION

The new resonance  $X(3872)$  has been discovered a few years ago by Belle [1] and has been later confirmed by the CDF [2], D0 [3] and *BABAR* [4] collaborations. It is classified as an isosinglet state with positive charge parity. Current averaged results for the  $X(3872)$  mass and width are:  $m_X = 3872.2 \pm 0.8$  MeV and  $\Gamma_X = 3.0_{-1.4}^{+1.9} \pm 0.9$  MeV [5]. For the  $X(3872)$  several structure interpretations have been proposed in the literature (for a status report see e.g. Refs. [6–8]). In the context of molecular approaches [9]–[33] the  $X(3872)$  can be identified with a weakly-bound hadronic molecule whose constituents are  $D$  and  $D^*$  mesons. The reason for this natural interpretation is that  $m_X$  is very close to the  $D^0\bar{D}^{*0}$  threshold and hence is in analogy to the deuteron — a weakly-bound state of proton and neutron. Note, that the idea to treat charmonium-like states as hadronic molecules traces back to Refs. [9, 10]. Originally it was proposed that the state  $X(3872)$  is a superposition of  $D^0\bar{D}^{*0}$  and  $\bar{D}^0D^{*0}$  pairs. Later (see e.g. discussion in Refs. [17, 19, 20]) also other structures, such as a charmonium state or even other meson pair configurations, were discussed in addition to the  $D^0\bar{D}^{*0}$  + charge conjugate (c.c.) component. The possibility of two nearly degenerated  $X(3872)$  states with positive and negative charge parity has been discussed in Refs. [26, 34].

In several papers [12, 29, 31, 33] the possibility that the  $X(3872)$  can be interpreted as a hadronic molecule — a bound state of  $D^0$  and  $D^{*0}$  mesons — has been investigated in potential models. These approaches can be traced back to Ref. [11], where possible deuteron-like two-meson bound states have been considered in the context of a potential generated by the pion exchange mechanism. It was shown that bound states of two mesons are possible in analogy to a deuteron model with one-pion exchange only. In addition, the relevance of the tensor interaction has been pointed out [11] which connects different spin-orbit configurations. These tensorial terms were found to be important to generate bound states in the potential model of the deuteron with a reasonable value for the cutoff  $\Lambda$ , which is a parameter regularizing the hadronic interaction. The value of  $\Lambda$  is determined phenomenologically and depends on the model, though its scale in low-energy hadron physics is of the order of 1 GeV. Later, after the discovery of the  $X(3872)$ , Tornqvist also showed [12] the importance of isospin breaking effects in a possible binding mechanism because of the mass differences between the neutral and charged  $D(D^*)$  mesons. Thomas and Close reinvestigated [31] in the context of one-pion exchange if the  $X(3872)$  can be a  $J^P = 1^+ DD^*$  bound state including charged mode and  $D$ -wave configurations. They also point out technical differences with respect to previous approaches, but moderate binding depends rather sensitively on the parameters involved. However, Liu *et al.* [29] claim that when taking into account both pion and also sigma meson exchange potentials the  $D$  and  $D^*$  mesons cannot form a bound state with reasonable values for the potential parameters. They show that a bound state is not present for values of  $\Lambda < 5.8$  GeV, where the upper value is too large compared to the typical hadronic scale of  $\Lambda \simeq 1$  GeV. But in their calculation

---

\* E-mail: ian-woo.lee@student.uni-tuebingen.de

† On leave of absence from Department of Physics, Tomsk State University, 634050 Tomsk, Russia

only the  $S$ -wave configuration was taken into account. Moreover, only the interaction transitions  $D^0\bar{D}^{*0} \rightarrow D^{*0}\bar{D}^0$  involving neutral  $D$  mesons were considered. This causes that the interaction strength is reduced by a factor of  $1/3$  compared to that of the isoscalar state in the isospin symmetry limit. Later, Liu *et al.* [33] showed that the  $X(3872)$  is open to the possibility of a loose bound state of  $D\bar{D}^*$  when one considers the isospin symmetry limit with  $I = 0$  and also when further heavy meson-exchange, such as  $\rho$  or  $\omega$  exchange, are included. Again, they restricted the calculation to the  $S$ -wave component and to the isospin symmetry limit.

The main objective of the present work is to improve the description of the  $X(3872)$  as a possible bound state of  $D$  and  $D^*$  mesons in the context of the potential model considered previously in Refs. [11, 12, 29, 31, 33]. In particular, we first consider a full set of mesons ( $\pi$ ,  $\sigma$ ,  $\eta$ ,  $\rho$  and  $\omega$ ) in constructing the nonrelativistic one-meson exchange potential, then we include charged and neutral  $D\bar{D}^*$  components both in orbital  $S$ - and  $D$ -waves. Full account is taken of isospin breaking effects by incorporating mass differences in the  $D$  and  $D^*$  mesons. As in the preceding papers we also regularize the potential by introducing form factors containing the cutoff parameter  $\Lambda$ .

In the manuscript we proceed as follows. First, in Sec. II we discuss the basic notions of our approach. We define the effective meson Lagrangian based on heavy hadron chiral perturbation theory, which then is used for the derivation of the meson-exchange potential in coordinate space. The formalism is developed to explicitly consider  $S$ - $D$  wave mixing and also to include isospin-symmetry breaking effects. In Sec. III we first discuss the numerical procedure for solving the coupled-channel Schroedinger equation. Then we present our results for a possible binding of the  $D\bar{D}^*$  system, discussing the influence of various components both in the potential and the di-meson configuration. In Section IV we extend our approach to the  $BB^*$  bound state system as well. Finally, in Sec. V, we present a short summary of our results and some general comments.

## II. METHOD

### A. Effective Lagrangian

Our starting point (as in the potential approach pursued in Refs. [29, 33]) is the effective Lagrangian of heavy hadron chiral perturbation theory (HHChPT) [35, 36] based on chiral and heavy quark symmetries. It gives rise to the interaction Lagrangians between  $D(D^*)$  mesons and light pseudoscalar, scalar and vector mesons with

$$\begin{aligned}
\mathcal{L}_{\mathcal{D}\mathcal{D}^*\mathbb{P}} &= -ig_{\mathcal{D}\mathcal{D}^*\mathbb{P}}(\mathcal{D}_a\mathcal{D}_{\mu b}^{*\dagger} - \mathcal{D}_{\mu a}^*\mathcal{D}_b^\dagger)\partial^\mu\mathbb{P}_{ab}, \\
\mathcal{L}_{\mathcal{D}\mathcal{D}^*\mathbb{V}} &= -2f_{\mathcal{D}\mathcal{D}^*\mathbb{V}}\varepsilon_{\mu\nu\alpha\beta}(\partial^\mu\mathbb{V}^\nu)_{ab}[(\mathcal{D}_a^\dagger\partial^\alpha\mathcal{D}_b^{*\beta} - \partial^\alpha\mathcal{D}_a^\dagger\mathcal{D}_b^{*\beta}) - (\mathcal{D}_a^{*\beta\dagger}\partial^\alpha\mathcal{D}_b - \partial^\alpha\mathcal{D}_a^{*\beta\dagger}\mathcal{D}_b)], \\
\mathcal{L}_{\mathcal{D}\mathcal{D}\sigma} &= -2m_{\mathcal{D}}g_\sigma\mathcal{D}_a\mathcal{D}_a^\dagger\sigma, \\
\mathcal{L}_{\mathcal{D}^*\mathcal{D}^*\sigma} &= 2m_{\mathcal{D}^*}g_\sigma\mathcal{D}_a^{*\alpha}\mathcal{D}_{\alpha a}^{*\dagger}\sigma, \\
\mathcal{L}_{\mathcal{D}\mathcal{D}\mathbb{V}} &= -ig_{\mathcal{D}\mathcal{D}\mathbb{V}}(\mathcal{D}_a^\dagger\partial_\mu\mathcal{D}_b - \mathcal{D}_b\partial_\mu\mathcal{D}_a^\dagger)(\mathbb{V}^\mu)_{ab}, \\
\mathcal{L}_{\mathcal{D}^*\mathcal{D}^*\mathbb{V}} &= ig_{\mathcal{D}^*\mathcal{D}^*\mathbb{V}}(\mathcal{D}_a^{*\nu\dagger}\partial^\mu\mathcal{D}_{\nu,b}^* - \mathcal{D}_{\nu,b}^*\partial^\mu\mathcal{D}_a^{*\nu\dagger})(\mathbb{V}_\mu)_{ab} + 4if_{\mathcal{D}^*\mathcal{D}^*\mathbb{V}}\mathcal{D}_{\mu,a}^{*\dagger}\mathcal{D}_{\nu,b}^*(\partial^\mu\mathbb{V}^\nu - \partial^\nu\mathbb{V}^\mu)_{ab},
\end{aligned} \tag{1}$$

where  $\mathcal{D}^{(*)} = (D^{0(*)}, D^{+(*)}, D_s^{+(*)})$ . The octet pseudoscalar  $\mathbb{P}$  and the nonet vector  $\mathbb{V}$  meson matrices are defined as

$$\mathbb{P} = \begin{pmatrix} \frac{\pi^0}{\sqrt{2}} + \frac{\eta}{\sqrt{6}} & \pi^+ & K^+ \\ \pi^- & -\frac{\pi^0}{\sqrt{2}} + \frac{\eta}{\sqrt{6}} & K^0 \\ K^- & \bar{K}^0 & -\frac{2\eta}{\sqrt{6}} \end{pmatrix} \tag{2}$$

and

$$\mathbb{V} = \begin{pmatrix} \frac{\rho^0}{\sqrt{2}} + \frac{\omega}{\sqrt{2}} & \pi^+ & K^{*+} \\ \rho^- & -\frac{\rho^0}{\sqrt{2}} + \frac{\omega}{\sqrt{2}} & K^{*0} \\ K^{*-} & \bar{K}^{*0} & \phi \end{pmatrix}. \tag{3}$$

The HHChPT couplings are given as

$$\begin{aligned}
g_{\mathcal{D}\mathcal{D}^*\mathbb{P}} &= \frac{2g}{f_\pi}\sqrt{m_{\mathcal{D}}m_{\mathcal{D}^*}}, \quad g_{\mathcal{D}\mathcal{D}\mathbb{V}} = g_{\mathcal{D}^*\mathcal{D}^*\mathbb{V}} = \frac{\beta g_{\mathbb{V}}}{\sqrt{2}}, \\
f_{\mathcal{D}\mathcal{D}^*\mathbb{V}} &= \frac{f_{\mathcal{D}^*\mathcal{D}^*\mathbb{V}}}{m_{\mathcal{D}^*}} = \frac{\lambda g_{\mathbb{V}}}{\sqrt{2}}, \quad g_{\mathbb{V}} = \frac{m_\rho}{f_\pi}, \quad g_\sigma = \frac{g_\pi}{2\sqrt{6}}, \\
g &= 0.59, \quad \beta = 0.9, \quad \lambda = 0.56 \text{ GeV}^{-1}, \quad f_\pi = 132 \text{ MeV}, \quad g_\pi = 3.73.
\end{aligned} \tag{4}$$

We assume that the  $X(3872)$  is a bound state of  $D^*$  and  $D$  with quantum numbers  $J^{PC} = 1^{++}$ . To compose a  $1^{++}$  state with a pseudoscalar and a vector meson, the orbital angular momentum can have the values of  $L = 0$  and 2. The leading-order meson exchange diagrams constructed with the use of these Lagrangians are shown in Figs. 1 (pseudoscalar-vector direct channels) and 2 (pseudoscalar-vector crossed channels). All diagrams are fixed to conserve angular momentum and parity. In the isospin symmetry limit, where  $D^{(*)0}$  and  $D^{(*)\pm}$  have no mass difference, the  $X(3872)$  can be represented explicitly as

$$|X\rangle = \frac{1}{2}[(|D^0\bar{D}^{*0}\rangle - c|D^{*0}\bar{D}^0\rangle) \pm (|D^+D^{*-}\rangle - c|D^{*+}D^-\rangle)] \quad (5)$$

where the  $\pm$  sign is determined according to the total isospin. The  $+$  sign corresponds to the isovector state and the  $-$  sign to the isoscalar one; the sign  $c = \pm 1$  adjusts even and odd charge conjugation parity, respectively. Here we use the convention where the vector field changes sign after charge conjugation. (for a detailed discussion about this issue and conventions used in literature see Refs. [29, 31]).

### B. Effective potentials in the direct channels

The effective potentials in momentum space are derived for the direct channels as follows :

$$V_{\text{dir}}(q) = g_\sigma^2 \frac{1}{q^2 - m_\sigma^2} - \frac{\gamma}{2} g_{\mathcal{D}\mathcal{D}\mathcal{V}} g_{\mathcal{D}^*\mathcal{D}^*\mathcal{V}} \left[ \frac{1}{q^2 - m_\rho^2} + \frac{q^2}{4m_D m_{D^*} m_\rho^2} \right] + \frac{1}{2} g_{\mathcal{D}\mathcal{D}\mathcal{V}} g_{\mathcal{D}^*\mathcal{D}^*\mathcal{V}} \left[ \frac{1}{q^2 - m_\omega^2} + \frac{q^2}{4m_D m_{D^*} m_\omega^2} \right] \quad (6)$$

where  $\gamma = 1$  and  $-3$  corresponds to the isovector and isoscalar channel, respectively. To avoid the singular behavior at small distances we further regularize the potential with a form factor  $F(q^2) = \frac{\Lambda^2 - m^2}{\Lambda^2 - q^2}$  ( $m$  is the mass of the exchanged meson) at each vertex. The value of the parameter  $\Lambda$  is not strictly determined. It should be about 1 GeV (a typical scale in low-energy physics) though its specific value can depend on the particular application. A larger value of  $\Lambda$  enhances the potential at short distances hence possible binding energies will depend on  $\Lambda$  as we shall discuss in Sec. IV.

The potentials in coordinate space can be obtained by Fourier transformation :

$$V_{\text{dir}}(r) = -\kappa_1 V_0 P_\sigma(r) + \gamma[\kappa_2 V_0 P_\rho(r) + \kappa_3 V_0 Q_\rho(r)] - [\kappa_2 V_0 P_\omega(r) + \kappa_3 V_0 Q_\omega(r)] \quad (7)$$

with the radial dependence

$$P_M(r) = \frac{m_\rho^2}{m_\pi^2} \left( \frac{e^{-\mu_M r} - e^{-\chi r}}{m_\pi r} - \frac{\Lambda^2 - m_M^2}{2m_\pi \chi} e^{-\chi r} \right), \quad (8)$$

$$Q_M(r) = \frac{1}{m_\pi^3 m_M^2} (\Lambda^2 - m_M^2)^2 \left( 1 - \frac{\Lambda^2}{2\chi} r \right) \frac{e^{-\chi r}}{r}, \quad (9)$$

where  $\mu_M^2 = m_M^2 - (m_{1'} - m_1)^2$  and  $\chi^2 = \Lambda^2 - (m_{1'} - m_1)^2$ . The subscripts at  $P$  and  $Q$  in Eq. (7) refer to the corresponding exchanged meson of mass  $m_M$ . Here we also define the constant  $V_0$

$$V_0 \equiv \frac{m_\pi^3 g^2}{12\pi f_\pi^2}, \quad (10)$$

which was already used in Refs. [11, 31]. This quantity is introduced to compare the strength of the one-pion exchange potential to the counterparts from the exchange of other scalar and vector mesons. The relevant strength coefficients are listed in the following. They are all dimensionless and the dimension of the potential is carried by  $V_0$ :

$$\kappa_1 = \frac{1}{8} \frac{g_\pi^2 f_\pi^2}{g^2 m_\rho^2} \simeq 0.146, \quad (11)$$

$$\kappa_2 = \frac{3}{4} \frac{\beta^2}{g^2} \simeq 1.75, \quad (12)$$

$$\kappa_3 = \frac{3}{16} \frac{\beta^2 m_\rho^2}{g^2 m_D m_{D^*}} \simeq 0.070. \quad (13)$$

### C. Effective potentials in the crossed channels

In the crossed channels we get the following effective potential in momentum space:

$$V_{\text{cross}}(q) = -\gamma c \frac{g_{\mathcal{D}\mathcal{D}^*\mathbb{P}}^2}{24m_{\mathcal{D}}m_{\mathcal{D}^*}} \frac{3(\vec{\varepsilon}_1 \cdot \vec{q})(\vec{\varepsilon}_{2'}^* \cdot \vec{q})}{q^2 - m_{\pi}^2} + c \frac{g_{\mathcal{D}\mathcal{D}^*\mathbb{P}}^2}{72m_{\mathcal{D}}m_{\mathcal{D}^*}} \frac{3(\vec{\varepsilon}_1 \cdot \vec{q})(\vec{\varepsilon}_{2'}^* \cdot \vec{q})}{q^2 - m_{\eta}^2} \\ + 2\gamma c f_{\mathcal{D}\mathcal{D}^*\mathbb{V}}^2 \frac{\vec{q}^2(\vec{\varepsilon}_1 \cdot \vec{\varepsilon}_{2'}^*) - (\vec{\varepsilon}_1 \cdot \vec{q})(\vec{\varepsilon}_{2'}^* \cdot \vec{q})}{q^2 - m_{\rho}^2} - 2c f_{\mathcal{D}\mathcal{D}^*\mathbb{V}}^2 \frac{\vec{q}^2(\vec{\varepsilon}_1 \cdot \vec{\varepsilon}_{2'}^*) - (\vec{\varepsilon}_1 \cdot \vec{q})(\vec{\varepsilon}_{2'}^* \cdot \vec{q})}{q^2 - m_{\omega}^2} \quad (14)$$

where  $\vec{\varepsilon}_1$  and  $\vec{\varepsilon}_{2'}^*$  are the polarization vectors of ingoing and outgoing vector mesons, respectively.

The quantity  $c = \pm 1$ , related to charge conjugation in Eq. (5), appears in every crossed diagram, which is different from the direct channels. The crossed channel potentials in coordinate space are obtained in similar manner as in the previous case:

$$V_{\text{cross}}(r) = c \left\{ -\frac{\gamma}{2} V_0 [C_{\pi}^-(r) + S_{12} T_{\pi}^-(r)] + \frac{1}{6} V_0 [C_{\eta}^+(r) + S_{12} T_{\eta}^+(r)] \right. \\ \left. + \kappa_4 \gamma V_0 [C_{\rho}^+(r) - \frac{1}{2} S_{12} T_{\rho}^+(r)] - \kappa_4 V_0 [C_{\omega}^+(r) - \frac{1}{2} S_{12} T_{\omega}^+(r)] \right\}, \quad (15)$$

where

$$C^+(r) = \frac{\mu^2}{m_{\pi}^2} \frac{e^{-\mu r} - e^{-\chi r}}{m_{\pi} r} - \frac{\chi(\Lambda^2 - m^2)}{2m_{\pi}^3} e^{-\chi r}, \quad (16)$$

$$T^+(r) = (\mu^2 r^2 + 3\mu r + 3) \frac{e^{-\mu r}}{m_{\pi}^3 r^3} - (\chi^2 r^2 + 3\chi r + 3) \frac{e^{-\chi r}}{m_{\pi}^3 r^3} - \frac{\Lambda^2 - m^2}{m_{\pi}^2} (\chi r + 1) \frac{e^{-\chi r}}{2m_{\pi} r}, \quad (17)$$

$$S_{12} = 3(\vec{\varepsilon}_1 \cdot \hat{r})(\vec{\varepsilon}_{2'}^* \cdot \hat{r}) - (\vec{\varepsilon}_1 \cdot \vec{\varepsilon}_{2'}^*). \quad (18)$$

Here  $m$  is the mass of the exchanged meson;  $\mu$  and  $\chi$  are defined as  $\mu^2 = m^2 - (m_{\mathcal{D}^*} - m_{\mathcal{D}})^2$  and  $\chi^2 = \Lambda^2 - (m_{\mathcal{D}^*} - m_{\mathcal{D}})^2$ , respectively;  $C^+$  and  $T^+$  are the potentials for positive values of  $\mu^2$ . In the case of  $\pi$  exchange, especially for  $\pi^0$  exchange, the mass of  $\pi^0$  is smaller than the mass difference ( $m_{\mathcal{D}^*} - m_{\mathcal{D}}$ ) so that  $\mu^2$  becomes negative. To take care of this case we define  $\bar{\mu}^2 = -\mu^2$  and obtain the real parts of these potentials as

$$C^-(r) = -\frac{\bar{\mu}^2}{m_{\pi}^2} \frac{\cos(\bar{\mu} r) - e^{-\chi r}}{m_{\pi} r} - \frac{\chi(\Lambda^2 - m^2)}{2m_{\pi}^3} e^{-\chi r}, \quad (19)$$

$$T^-(r) = (-\bar{\mu}^2 r^2 + 3) \frac{\cos(\bar{\mu} r)}{m_{\pi}^3 r^3} + 3\bar{\mu} r \frac{\sin(\bar{\mu} r)}{m_{\pi}^3 r^3} - (\chi^2 r^2 + 3\chi r + 3) \frac{e^{-\chi r}}{m_{\pi}^3 r^3} - \frac{\Lambda^2 - m^2}{m_{\pi}^2} (\chi r + 1) \frac{e^{-\chi r}}{2m_{\pi} r}. \quad (20)$$

$\Lambda$  is sufficiently large so that the sign of  $\chi^2$  is not affected by the sign of  $\mu^2$ .

The functions  $C^{\pm}$  and  $T^{\pm}$  are dimensionless and their shape depends on the value of  $\Lambda$  and the mass  $m$  of the exchanged mesons. To compare the strength of the potential due to vector meson exchange to the counterparts of the pseudoscalar mesons we define the dimensionless parameter  $\kappa_4$  as

$$\kappa_4 = \frac{4}{3} f_{\mathcal{D}^*\mathcal{D}\mathbb{V}}^2 \frac{3f_{\pi}^2}{g^2} = 2\lambda^2 \frac{m_{\rho}^2}{g^2} \simeq 1.07. \quad (21)$$

We present the potentials in the crossed channels again to see the tensorial terms clearly. Writing the potential in the  $L = 0, 2$  basis we have

$$V_{\text{cross}}(r) = V_0 \left[ \begin{pmatrix} 1 & 0 \\ 0 & 1 \end{pmatrix} C_{\text{cross}}(r) + \begin{pmatrix} 0 & -\sqrt{2} \\ -\sqrt{2} & 1 \end{pmatrix} T_{\text{cross}}(r) \right] \quad (22)$$

where

$$C_{\text{cross}}(r) = -\frac{\gamma}{2} C_{\pi}^-(r) + \frac{1}{6} C_{\eta}^+(r) + \gamma \kappa_4 C_{\rho}^+(r) - \kappa_4 C_{\omega}^+(r), \quad (23)$$

$$T_{\text{cross}}(r) = -\frac{\gamma}{2} T_{\pi}^-(r) + \frac{1}{6} T_{\eta}^+(r) - \frac{\gamma}{2} \kappa_4 T_{\rho}^+(r) + \frac{1}{2} \kappa_4 T_{\omega}^+(r). \quad (24)$$

Finally we get the total meson exchange potential, which is the sum of the potentials from the direct and crossed channels:

$$V_{\text{total}}(r) = V_{\text{dir}}(r) + V_{\text{cross}}(r). \quad (25)$$

The profile functions  $P(r)$ ,  $Q(r)$ ,  $C(r)$  and  $T(r)$  encoding the contribution of meson exchange to the potential are plotted in Fig.3. One can see that the functions  $C(r)$  and  $Q(r)$  dominate at small distances. Of course strength and range of all curves depend on the mass of the exchanged meson and the value of  $\Lambda$ , but Fig. 3 contains at least the characteristics of each function.  $V_0$  is fixed at 1.3 MeV (or 1.5 MeV) by the experimental data on the decay width  $\Gamma(D^{*+} \rightarrow D^0\pi^+)$ . We choose the value  $V_0=1.3$  MeV used before in Refs. [11, 31] which is also consistent with the parameters of the HHChPT Lagrangian (4).

Multiplying the relevant coefficients such as  $\kappa_1 V_0$ ,  $\kappa_2 V_0$ , etc. with  $P(r)$ ,  $Q(r)$ ,  $C(r)$  and  $T(r)$  in Fig. 4 we indicate the potentials in the isoscalar limit (that is, with  $\gamma = -3$ ). The total potential is written as

$$V_{total} = V_C \begin{pmatrix} 1 & 0 \\ 0 & 1 \end{pmatrix} + V_T \begin{pmatrix} 0 & -\sqrt{2} \\ -\sqrt{2} & 1 \end{pmatrix} \quad (26)$$

in the  $L = 0, 2$  basis. The tensor potential  $V_T = V_0 T_{\text{cross}}$  arises only from the crossed channels. The central potential  $V_C = V_{\text{dir}} + V_0 C_{\text{cross}}$  does not mix  $S$  and  $D$  waves. In Fig.4(a) we indicate the individual contributions to  $V_C$  and the total result for a cutoff in the form factors of  $\Lambda = 1250$  MeV. The contributions of  $\pi$  and  $\rho$  meson exchange are dominant and attractive. The effect of  $\sigma$ -exchange is small, though it depends on the  $\sigma$  mass. The vector meson potentials become slightly attractive around 0.1 - 0.2 fm but are negligible compared to the total potential. In Fig.4(b) we indicate the off-diagonal potential  $V_T$  including all exchanged mesons for  $\Lambda=1250$  MeV. The pseudoscalar and vector meson potentials have different sign, but the  $\pi$  contribution dominates such that the total potential becomes attractive. From Eq. (14) it is evident that the different signs of the pseudoscalar and vector meson potentials are dictated by the opposite sign in the effective Lagrangian. Not only  $V_C$  plays a possible role to generate attraction for the X state but also  $V_T$  though its strength is small compared to  $V_C$  at short distances.

#### D. Isospin symmetry breaking

We set up the  $X(3872)$  as a mixture of the isoscalar and the isovector components, that is  $|X\rangle = c_0|0\rangle + c_{\pm}|\pm\rangle$ , where  $|0\rangle = \frac{1}{\sqrt{2}}(|D^0\bar{D}^{*0}\rangle - c|D^{*0}\bar{D}^0\rangle)$  and  $|\pm\rangle = \frac{1}{\sqrt{2}}(|D^+\bar{D}^{*-}\rangle - c|D^{*+}\bar{D}^-\rangle)$ . In the limit of isospin symmetry the coefficients exactly fulfill the relation  $|c_0| = |c_{\pm}| = \frac{1}{\sqrt{2}}$ . The mass differences between the neutral and charged channel induce slight changes in these coefficients. When isospin symmetry is broken, the isoscalar factor  $\gamma = -3$  in the potentials should be replaced by a  $2 \times 2$  matrix

$$\begin{pmatrix} -1 & -2 \\ -2 & -1 \end{pmatrix} \quad (27)$$

in the particle basis of neutral  $|0\rangle$  and charged  $|\pm\rangle$  states. Here the diagonal matrix elements of  $-1$  come from the exchange of neutral mesons, while the off-diagonal matrix elements  $-2$  arise from charged meson exchange. We have four different potentials according to the corresponding diagrams. Then the Schrödinger equation becomes as follows:

$$\left[ \begin{pmatrix} M_0 - \frac{\nabla^2}{2m_0} & 0 \\ 0 & M_{\pm} - \frac{\nabla^2}{2m_{\pm}} \end{pmatrix} + \begin{pmatrix} -V_a & -2V_c \\ -2V_d & -V_b \end{pmatrix} \right] \begin{pmatrix} c_0|0\rangle \\ c_{\pm}|\pm\rangle \end{pmatrix} = E \begin{pmatrix} c_0|0\rangle \\ c_{\pm}|\pm\rangle \end{pmatrix}, \quad (28)$$

where  $m_0$  and  $m_{\pm}$  are the reduced masses while  $M_0$ ,  $M_{\pm}$  are the total masses of neutral and charged systems, respectively. Here, for example,  $V_a$  is the potential which is generated by the diagrams (a) in Figs.1 and 2 with

$$V_a = \begin{pmatrix} 1 & 0 \\ 0 & 1 \end{pmatrix} V_a^{\text{dir}} + \left[ \begin{pmatrix} 1 & 0 \\ 0 & 1 \end{pmatrix} V_0 C_a^{\text{cross}} + \begin{pmatrix} 0 & -\sqrt{2} \\ -\sqrt{2} & 1 \end{pmatrix} V_0 T_a^{\text{cross}} \right] \quad (29)$$

in the  $L = 0, 2$  basis. Accordingly,  $V_{b,c,d}$  are due to the corresponding graphs of Figs.1 and 2.

### III. RESULTS

#### A. Numerical method

To get solutions to the Schrödinger equation with the derived potential we need to solve coupled second-order differential equations. The numerical procedure is as follows: we discretize  $r$ -space and diagonalize the potential at each discretized position with the boundary conditions that both  $S$  and  $D$  waves vanish at  $r \rightarrow \infty$ . Then the

Hamiltonian becomes a finite matrix and we solve the Schrödinger equation using diagonalization routines. This method is well suited for obtaining the ground state wave function and eigenvalue in the bound system. We tested the results varying the values of the boundary position and the number of discretization points.

To confirm our numerical calculations we also adopt another method in solving the Schrödinger equation by using MATSCS, which is a Matlab package implementing the CPM{P,N} methods for the numerical solution of the multichannel Schrödinger eigenvalue problem [37]. We obtain agreement in the results for the energy eigenvalue within 0.1 MeV between our matrix method and MATSCS. This double check can only be performed in the limit of isospin symmetry, because MATSCS can only solve symmetric potentials. When isospin symmetry is broken the multichannel potentials are slightly distorted and do not coincide any more for the neutral and the charged states.

## B. Results

In Table I we summarize our results for the binding energy  $E_{\text{bin}} = E - M_0$  ( $M_0$  is the total mass of the neutral component) in dependence on the form factor cutoff  $\Lambda$ . In addition we also indicate the probabilities  $P$  for having the neutral  $|0\rangle$  or the charged  $|\pm\rangle$  components either in  $S$ - or  $D$ -wave in the bound state wave function. The size of the system is characterized by the rms radius of the dominant neutral  $S$ -wave component.

As  $\Lambda$  is growing the binding energy becomes larger. This is expected since the attractive potentials get stronger when  $\Lambda$  is growing. The ratio between the neutral and the charged states is very sensitive to the explicit value of  $\Lambda$ . The isospin-breaking effect mainly comes from the mass difference between the neutral and the charged  $D\bar{D}^*$  system, that is  $M_{\pm} - M_0 \approx 8.1$  MeV. The corresponding wave functions at a binding energy of  $-0.40$  MeV are shown in Fig.5. The neutral states dominate and the  $D$ -wave components are negligible. In Fig.6 we also present the corresponding probabilities near  $|E_{\text{bin}}| \approx 0$ . When the binding energy become larger, however, the effect of the mass difference between neutral and charged states weakens and the isospin symmetry is almost restored. For example, at a value of  $\Lambda=2500$  MeV the binding energy is  $-555.34$  MeV, which by its absolute value is larger than 8.1 MeV. For this value of  $\Lambda$  the probabilities  $P(0_S), P(0_D), P(\pm_S)$  and  $P(\pm_D)$  are 46.1, 4.2, 45.6 and 4.1, respectively.

In Table II we indicate our results in the isospin limit. Compared with the full case of Table I the isospin-breaking effects reduce  $\Lambda$  by about 90 MeV to obtain a bound state with the same binding energy. The isovector state of  $D\bar{D}^*$  cannot make a bound state while the isoscalar state can and mixing of isovector and isoscalar components leads to a weakening of the binding energy.

To identify the relevant components both in the potential and the bound  $D\bar{D}^*$  configuration we also looked at reduced variants of this approach. For example, when just keeping pion-exchange in the potential a bound state can be formed for values of  $\Lambda \geq 1700$  MeV. This result is consistent with the findings in Ref. [31]. Turning on in addition  $\sigma$  meson exchange slightly increases the binding energy with the effect depending on the explicit mass value  $m_{\sigma}$ . We vary the value of  $m_{\sigma}$  from 200 MeV to 600 MeV. When we consider  $\pi$  and  $\rho$  meson exchange we only get a bound state for values of  $\Lambda \geq 1250$  MeV. Further additional meson exchange components do not introduce a significant effect.

When we turn off the charged  $D\bar{D}^*$  components we assume that the X meson is no more isoscalar, but a bound state of neutral  $D^0\bar{D}^{*0}$  components only. Including in this case pion-exchange only leads to a minimal value of  $\Lambda = 4450$  MeV for the case of binding. Neglecting in addition the  $D$ -wave effect a bound state can only be generated for  $\Lambda \geq 5900$  MeV. These results fully agree with the ones of Ref. [29]. If we include all meson exchanges but still neglect the charged component a bound state is obtained at  $\Lambda = 2050$  MeV. Further neglect of the  $D$ -wave results in a minimal value of  $\Lambda = 2300$  MeV to form a bound state.

Switching off the  $D$ -wave results in a binding energy of  $-0.23$  MeV at  $\Lambda = 1250$  MeV. This value of  $-0.23$  MeV is smaller than the value of  $-6.32$  MeV which is obtained in the full calculation. Thus we conclude that to form a bound state the condition of  $I = 0$  plays an important role as well as  $\pi$  and  $\rho$  meson exchanges, but  $S - D$  wave mixing effect is less significant.

## IV. $BB^*$ BOUND STATES

Heavy quark symmetry and the nonrelativistic approximation is more reliable for heavy-light systems containing a  $b$  instead of a  $c$  quark. From this point of view it is worthwhile to study if in analogy to the  $DD^*$  system  $B$  and  $B^*$  mesons can also form molecular bound states. In Table III we indicate possible  $BB^*$  bound states in dependence on  $\Lambda$ . The mass values of  $m_B=5279.4$  MeV and  $m_{B^*}=5325.0$  MeV are used as input. The mass differences between the neutral and charged  $B^{(*)}$  mesons are not known experimentally at the moment. Therefore, isospin-breaking effects only arise from the mass differences of the exchanged mesons such as  $\pi$  or  $\rho$ . However, these mass differences for the exchanged mesons cause very slight deformation in the potential and its effect is negligible. Presently it is the best option to assume isospin symmetry.

We calculate combinations of possible  $B\bar{B}^*$  bound states assumed to be an isoscalar or an isovector with charge parity even or odd.  $B\bar{B}^*$  is likely to form a bound state both with  $J^{PC} = 1^{++}$  and  $1^{+-}$  in the isoscalar limit for reasonable values of  $\Lambda$ . In the case of  $DD^*$  no bound state with  $J^{PC} = 1^{+-}$  is possible for a suitable value of  $\Lambda$ . Compared to the  $D\bar{D}^*$  case the heavier mass of the  $B\bar{B}^*$  states leads to a reduction of momentum and hence of the angular momentum terms which act repulsive, and therefore binding becomes easier.

As evident from the first part (related to  $J^{PC} = 1^{++}$ ) of Table III binding energies even increase for reduced values of  $\Lambda < 700$  MeV. As a matter of fact the parameter  $\Lambda$  was introduced to regularize the attractive delta-function in the effective potential. The potential becomes deeper as  $\Lambda$  increases with the form factor approaching 1 when  $\Lambda$  goes to infinity. However, as displayed in Fig.7(b) the potential gets deeper even when  $\Lambda$  becomes smaller. This effect happens when  $\Lambda$  is smaller than the mass of the exchanged meson. This might not have any significant physical meaning at this low  $\Lambda$  values, but it is questionable if one can simply ignore this behavior of a deepening potential at low  $\Lambda$ . Despite of this  $B\bar{B}^*$  bound states can be formed for a reasonable values of  $\Lambda$ , around 1 GeV, which is larger than the mass of the exchanged mesons.

## V. CONCLUSION

In this paper we explore the possibility to generate bound states with  $D$  and  $D^*$  mesons in a potential model. Using the HHChPT Lagrangian we construct the effective potential including isospin symmetry breaking and also S-D wave mixing. In this effective potential the whole light pseudoscalar and vector mesons play the role of exchange particles between  $D$  and  $D^*$  mesons. Because of the heavy mass of the  $D\bar{D}^*$  system a nonrelativistic approximation is meaningful. We therefore solve a coupled channel Schrödinger equation with specific potentials that are given by the effective Lagrangian. Binding of the  $D\bar{D}^*$  system is obtained for reasonable values of  $\Lambda \simeq 1.2$  GeV, increase of this cutoff value will generate deeper binding. Comparing this result to the isospin symmetry limit the  $DD^*$  bound state where isospin symmetry is broken needs a somewhat larger  $\Lambda$  but still within a reasonable range of values. By switching on and off various factors we also demonstrated that the relevant ingredients for binding are the  $I = 0$  condition and  $\pi$ ,  $\rho$  meson exchanges. The S-D wave mixing effect is essentially negligible.

We extended our method to the  $B\bar{B}^*$  system to see if a molecular bound state is possible. Bound states of  $B\bar{B}^*$  are formed both with  $J^{PC} = 1^{++}$  and  $1^{+-}$  in the isoscalar limit. But we find that it is harder to make a  $B\bar{B}^*$  bound state in the isovector limit just as for  $D\bar{D}^*$ . If the mass differences between the neutral and charged  $B^{(*)}$  were known, then we could apply our method to see if isospin breaking effects play an important role. But presently we assume isospin symmetry in calculating the binding energies of the  $B\bar{B}^*$ -system.

It is remarkable that there could be two different states in a molecular  $B\bar{B}^*$  picture: with  $J^{PC} = 1^{++}$  and  $1^{+-}$  (both with  $I = 0$ ). For example when  $\Lambda = 1000$  MeV the binding energy of  $1^{++}$  is  $-21.13$  MeV while that of  $1^{+-}$  is  $-0.34$  MeV. Future possible detection of these states can give strong support to the molecular approach in the heavy meson sector.

## Acknowledgments

This work was supported by the DFG under Contract No. FA67/31-2 and No. GRK683. This research is also part of the European Community-Research Infrastructure Integrating Activity ‘‘Study of Strongly Interacting Matter’’ (HadronPhysics2, Grant Agreement No. 227431) and of the President grant of Russia ‘‘Scientific Schools’’ No. 871.2008.2. The work is partially supported by Russian Science and Innovations Federal Agency under contract No 02.740.11.0238. We thank C. Thomas and V. Ledoux for helpful discussions on the numerical calculations.

- 
- [1] S. K. Choi *et al.* (Belle Collaboration), Phys. Rev. Lett. **91**, 262001 (2003) [arXiv:hep-ex/0309032].
- [2] D. E. Acosta *et al.* (CDF II Collaboration), Phys. Rev. Lett. **93**, 072001 (2004) [arXiv:hep-ex/0312021].
- [3] V. M. Abazov *et al.* (D0 Collaboration), Phys. Rev. Lett. **93**, 162002 (2004) [arXiv:hep-ex/0405004].
- [4] B. Aubert *et al.* [BABAR Collaboration], Phys. Rev. D **71**, 071103 (2005) [arXiv:hep-ex/0406022].
- [5] C. Amsler *et al.* (Particle Data Group), Phys. Lett. B **667**, 1 (2008).
- [6] E. S. Swanson, Phys. Rept. **429**, 243 (2006) [arXiv:hep-ph/0601110].
- [7] G. Bauer, Int. J. Mod. Phys. A **21**, 959 (2006) [arXiv:hep-ex/0505083].
- [8] M. B. Voloshin, Prog. Part. Nucl. Phys. **61**, 455 (2008) [arXiv:0711.4556 [hep-ph]].
- [9] M. B. Voloshin and L. B. Okun, JETP Lett. **23**, 333 (1976) [Pisma Zh. Eksp. Teor. Fiz. **23**, 369 (1976)].
- [10] A. De Rujula, H. Georgi and S. L. Glashow, Phys. Rev. Lett. **38**, 317 (1977).
- [11] N. A. Tornqvist, Z. Phys. C **61**, 525 (1994) [arXiv:hep-ph/9310247].
- [12] N. A. Tornqvist, Phys. Lett. B **590**, 209 (2004) [arXiv:hep-ph/0402237].
- [13] S. Pakvasa and M. Suzuki, Phys. Lett. B **579**, 67 (2004) [arXiv:hep-ph/0309294].
- [14] M. B. Voloshin, Phys. Lett. B **579**, 316 (2004) [arXiv:hep-ph/0309307].
- [15] E. Braaten and M. Kusunoki, Phys. Rev. D **69**, 074005 (2004) [arXiv:hep-ph/0311147].
- [16] F. E. Close and P. R. Page, Phys. Lett. B **578**, 119 (2004) [arXiv:hep-ph/0309253].
- [17] E. S. Swanson, Phys. Lett. B **588**, 189 (2004) [arXiv:hep-ph/0311229].
- [18] E. S. Swanson, Phys. Lett. B **598**, 197 (2004) [arXiv:hep-ph/0406080].
- [19] M. B. Voloshin, Phys. Lett. B **604**, 69 (2004) [arXiv:hep-ph/0408321].
- [20] E. Braaten and M. Kusunoki, Phys. Rev. D **72**, 054022 (2005) [arXiv:hep-ph/0507163].
- [21] M. T. AlFiky, F. Gabbiani and A. A. Petrov, Phys. Lett. B **640**, 238 (2006) [arXiv:hep-ph/0506141].
- [22] Yu. S. Kalashnikova, Phys. Rev. D **72**, 034010 (2005) [arXiv:hep-ph/0506270].
- [23] M. B. Voloshin, Int. J. Mod. Phys. A **21**, 1239 (2006) [arXiv:hep-ph/0509192].
- [24] X. Liu, B. Zhang and S. L. Zhu, Phys. Lett. B **645**, 185 (2007) [arXiv:hep-ph/0610278]; C. Meng and K. T. Chao, Phys. Rev. D **75**, 114002 (2007) [arXiv:hep-ph/0703205].
- [25] E. Braaten, M. Lu and J. Lee, Phys. Rev. D **76**, 054010 (2007) [arXiv:hep-ph/0702128].
- [26] D. Gamermann and E. Oset, Eur. Phys. J. A **33**, 119 (2007) [arXiv:0704.2314 [hep-ph]].
- [27] S. Fleming, M. Kusunoki, T. Mehen and U. van Kolck, Phys. Rev. D **76**, 034006 (2007) [arXiv:hep-ph/0703168].
- [28] E. Braaten and M. Lu, Phys. Rev. D **77**, 014029 (2008) [arXiv:0710.5482 [hep-ph]].
- [29] Y. R. Liu, X. Liu, W. Z. Deng and S. L. Zhu, Eur. Phys. J. C **56**, 63 (2008) [arXiv:0801.3540 [hep-ph]].
- [30] Y. B. Dong, A. Faessler, T. Gutsche and V. E. Lyubovitskij, Phys. Rev. D **77**, 094013 (2008) [arXiv:0802.3610 [hep-ph]]; Y. Dong, A. Faessler, T. Gutsche, S. Kovalenko and V. E. Lyubovitskij, Phys. Rev. D **79**, 094013 (2009); Y. Dong, A. Faessler, T. Gutsche and V. E. Lyubovitskij, arXiv:0909.0380 [hep-ph].
- [31] C. E. Thomas and F. E. Close, Phys. Rev. D **78**, 034007 (2008) [arXiv:0805.3653 [hep-ph]].
- [32] S. Fleming and T. Mehen, Phys. Rev. D **78**, 094019 (2008) [arXiv:0807.2674 [hep-ph]].
- [33] X. Liu, Z. G. Luo, Y. R. Liu and S. L. Zhu, arXiv:0808.0073 [hep-ph].
- [34] K. Terasaki, Prog. Theor. Phys. **118**, 821 (2007) [arXiv:0706.3944 [hep-ph]].
- [35] M. B. Wise, Phys. Rev. D **45**, R2188 (1992); G. Burdman and J. F. Donoghue, Phys. Lett. B **280**, 287 (1992). U. Kilian, J. G. Korner and D. Pirjol, Phys. Lett. B **288**, 360 (1992). A. F. Falk and M. E. Luke, Phys. Lett. B **292**, 119 (1992) [arXiv:hep-ph/9206241]; T. M. Yan, H. Y. Cheng, C. Y. Cheung, G. L. Lin, Y. C. Lin and H. L. Yu, Phys. Rev. D **46**, 1148 (1992) [Erratum-ibid. D **55**, 5851 (1997)]; H. Y. Cheng, C. Y. Cheung, G. L. Lin, Y. C. Lin, T. M. Yan and H. L. Yu, Phys. Rev. D **47**, 1030 (1993) [arXiv:hep-ph/9209262]; R. Casalbuoni, A. Deandrea, N. Di Bartolomeo, R. Gatto, F. Feruglio and G. Nardulli, Phys. Rept. **281**, 145 (1997) [arXiv:hep-ph/9605342].
- [36] C. Isola, M. Ladisa, G. Nardulli and P. Santorelli, Phys. Rev. D **68**, 114001 (2003) [arXiv:hep-ph/0307367].
- [37] V. Ledoux, M. Van Daele, G. Vanden Berghe, Comp. Phys. Comm. **176**, 191 (2007).



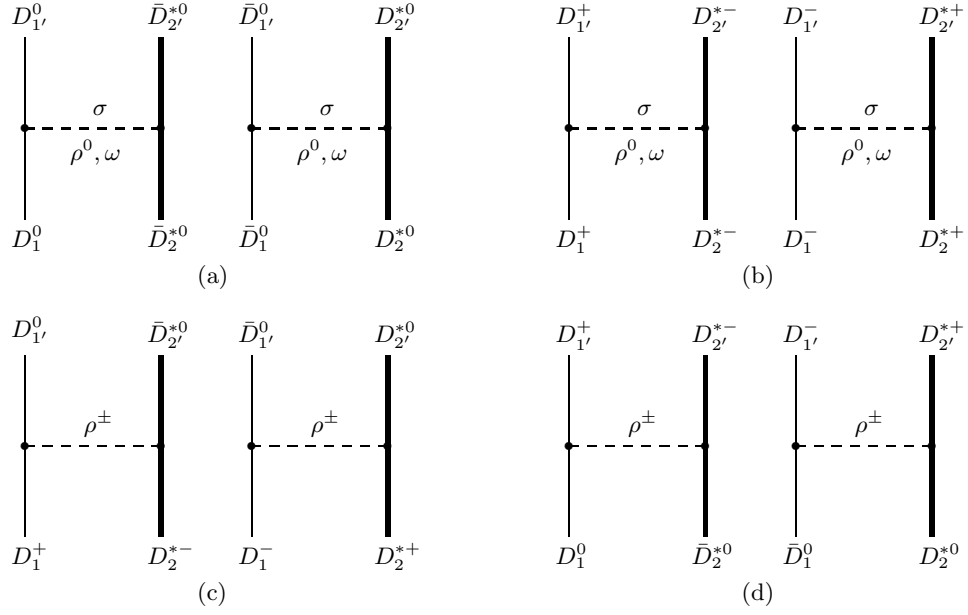


FIG. 1: Feynman diagrams describing the scattering of  $D$  and  $D^*$  in the pseudoscalar-vector direct channel: (a) and (b) – Isospin channel  $I = 0$  and the isotopic factors are equal to  $-1$ ; (c) and (d) – Isospin channel  $I = 1$  and the isotopic factors are equal to  $2$ . The bold (solid) lines stand for vector  $D^*$  (scalar  $D$ ) mesons while the dashed lines represent the exchanged mesons.

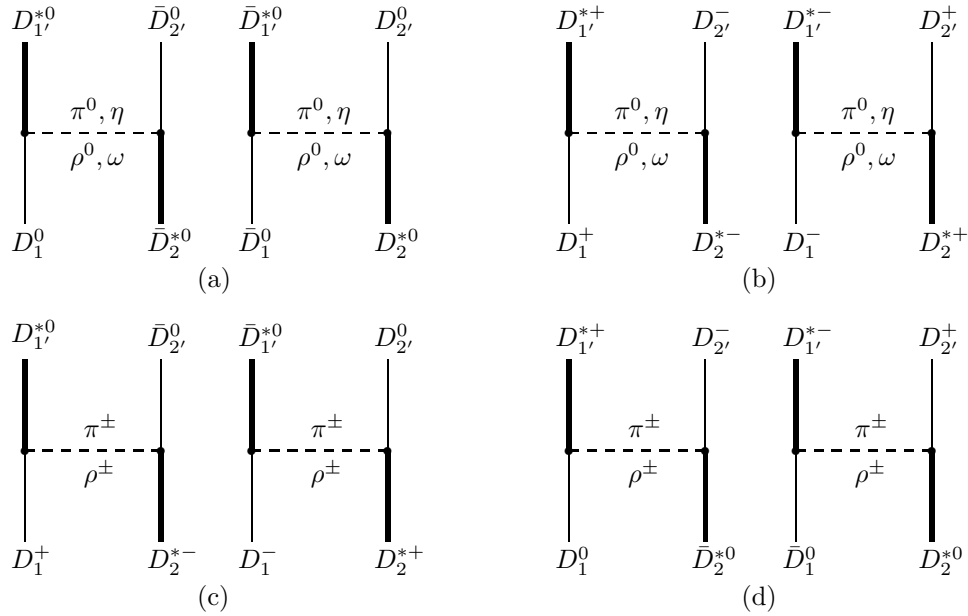


FIG. 2: Feynman diagrams describing the scattering of  $D$  and  $D^*$  in the pseudoscalar-vector crossed channel; (a) and (b) – Isospin channel  $I = 0$  and the isotopic factors are equal to  $-1$ ; (c) and (d) – Isospin channel  $I = 1$  and the isotopic factors are equal to  $2$ . The bold (solid) lines stand for vector (scalar) mesons while the dashed lines represent the exchanged mesons.

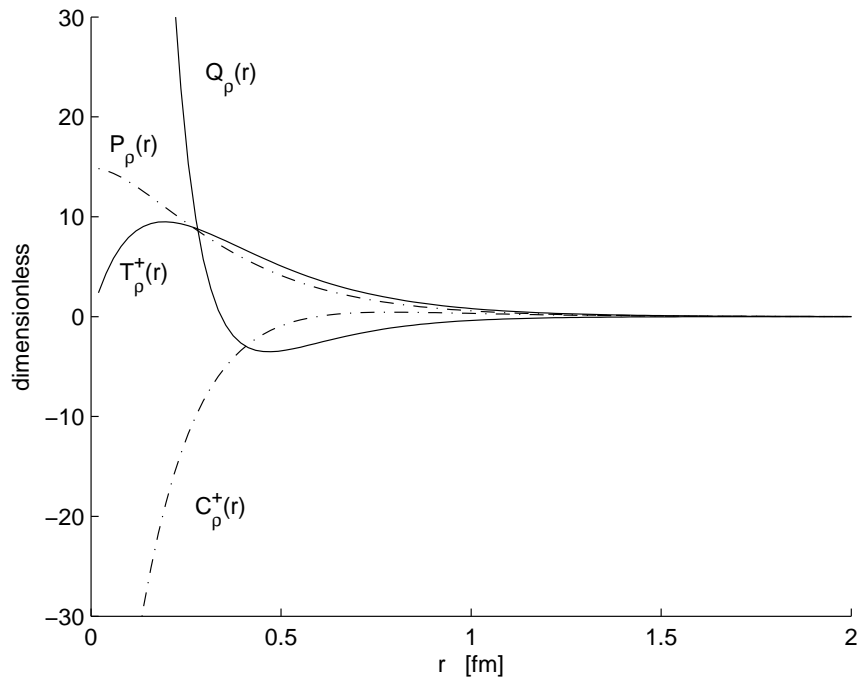
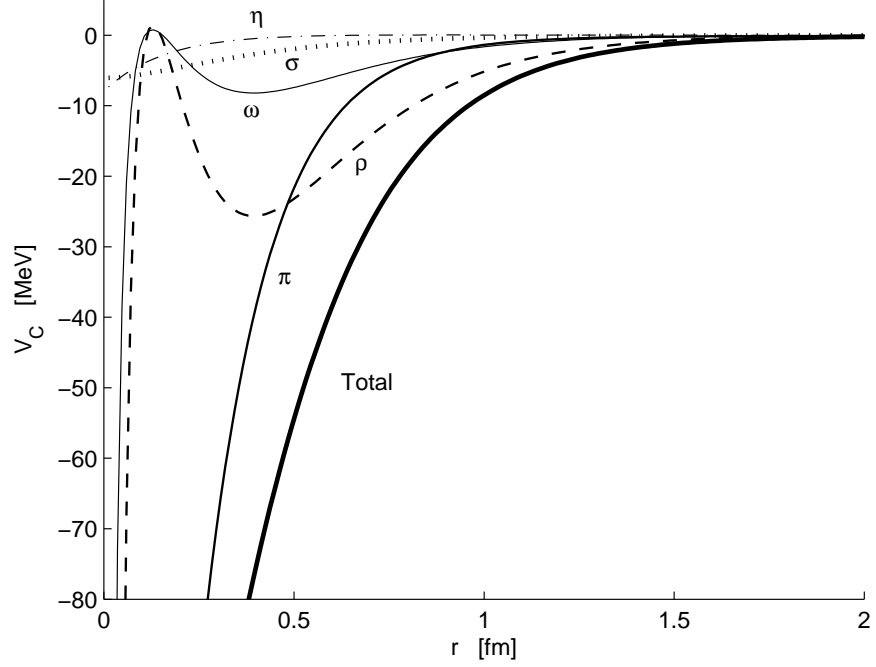
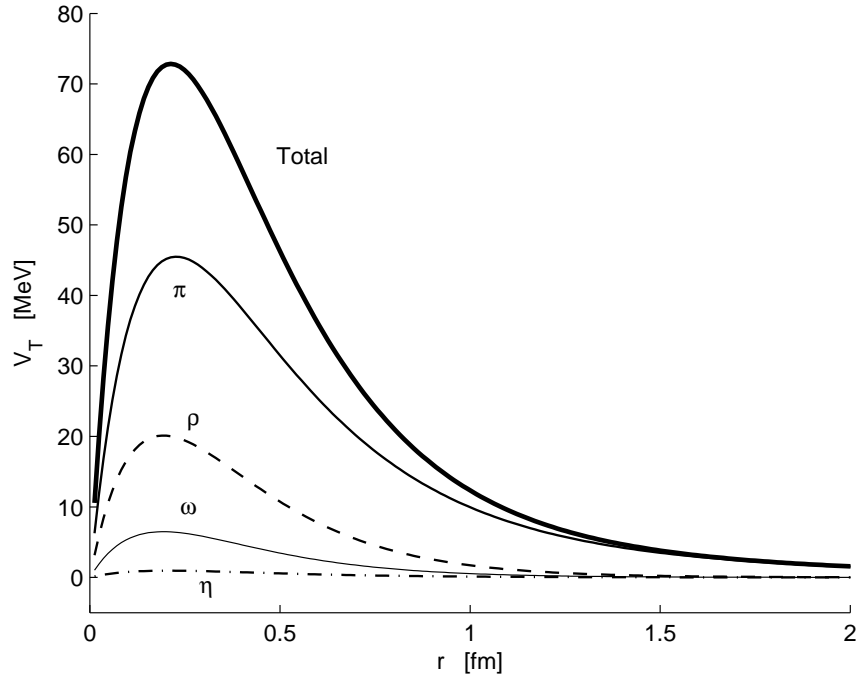


FIG. 3: Comparison of the shapes of the dimensionless potentials for  $\Lambda = 1250$  MeV. The mass value is chosen as the  $\rho$  meson mass,  $m = 771$  MeV.



(a)



(b)

FIG. 4: Central and tensor potentials due to meson-exchange for  $\Lambda=1250$  MeV.

(a) the central potentials  $V_C$  ( $\pi$  and  $\rho$  meson exchange is dominantly attractive); (b) the tensor potentials  $V_T$  due to the crossed channels ( $\pi$  and  $\rho$  mesons are dominant and equal in sign).

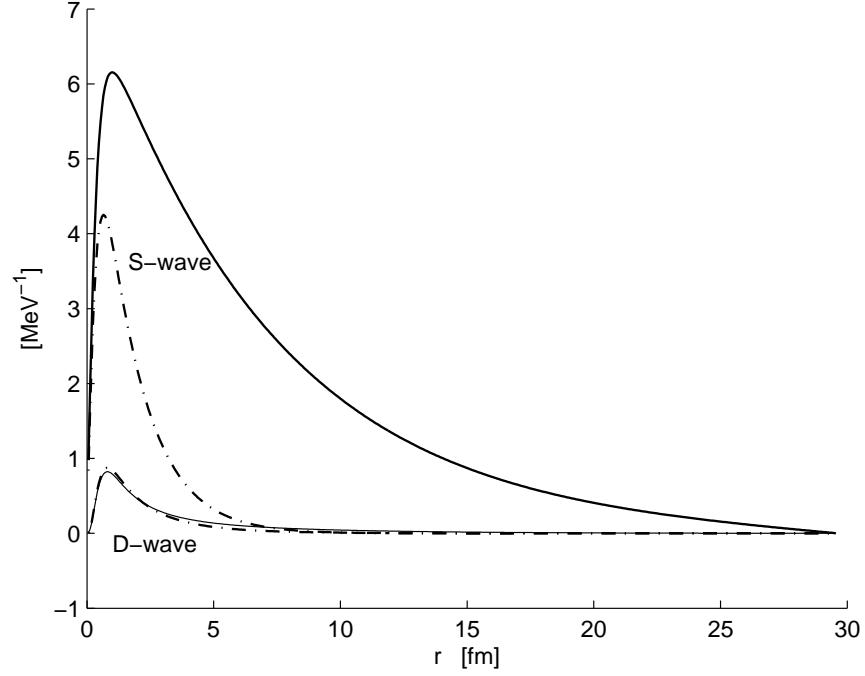


FIG. 5: Bound state wave function including isospin symmetry breaking for  $\Lambda=1250$  MeV. Bold lines denote the neutral states while dot-dashed lines denote the charged states.

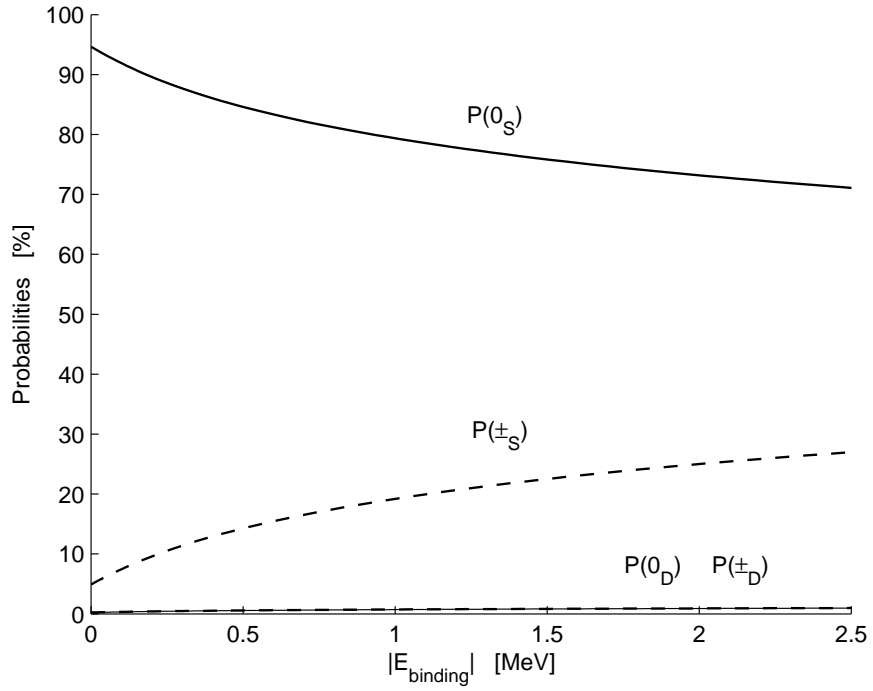
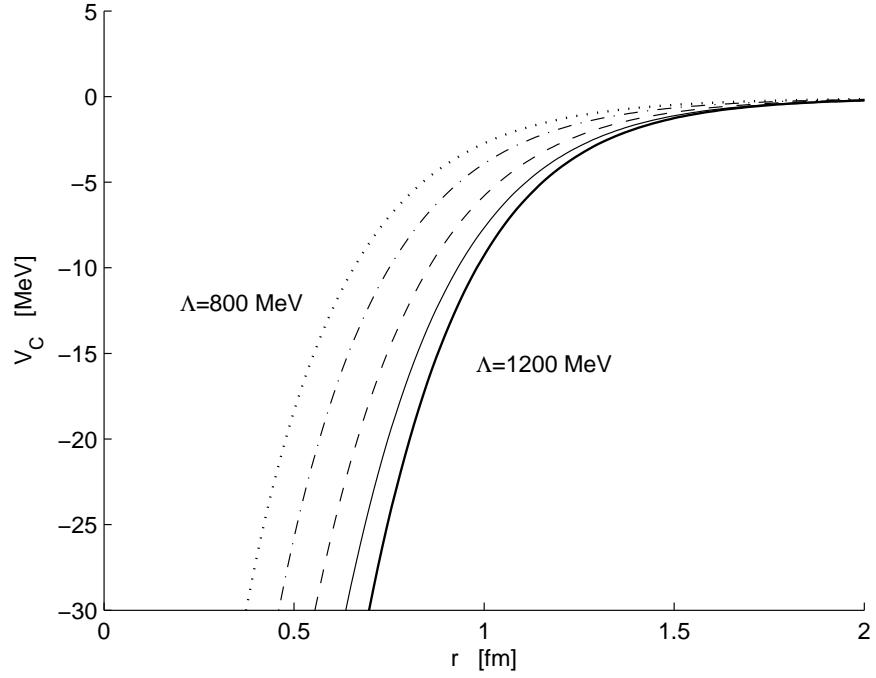
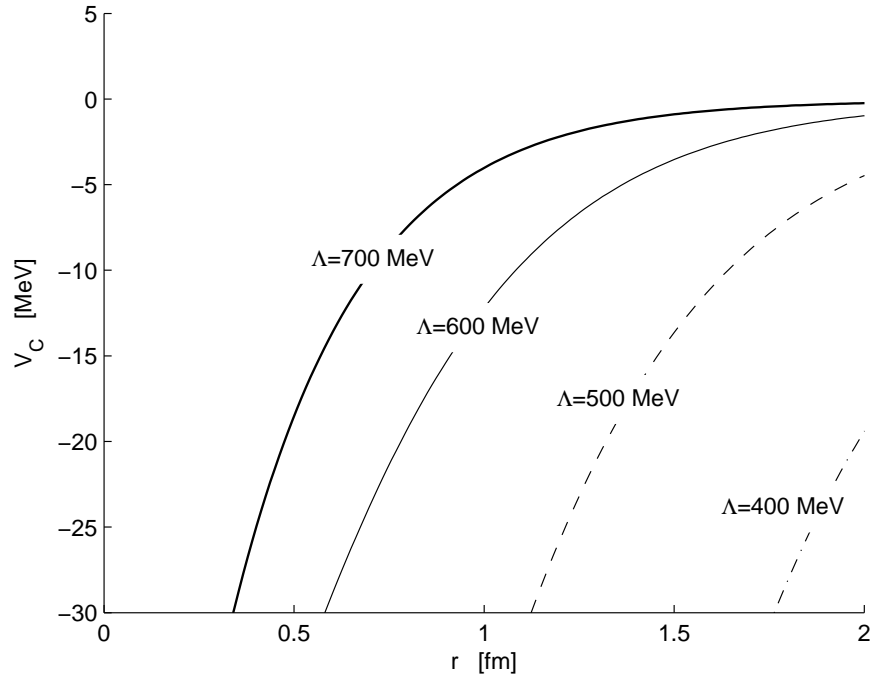


FIG. 6: The corresponding probabilities near  $|E_{\text{bin}}| \approx 0$ . Bold lines denote the neutral states while dot-dashed lines denote the charged states.



(a)



(b)

FIG. 7: The behavior of the central potentials for various values of  $\Lambda$ .

TABLE I: Binding energies with varying  $\Lambda$  in the isospin breaking case.

$\Lambda$ [MeV]	$E_{\text{bin}}$ [MeV]	$E = M_0 + E_{\text{bin}}$ [MeV]	$P(0_S)\%$	$P(0_D)\%$	$P(\pm_S)\%$	$P(\pm_D)\%$	rms( $0_S$ ) [fm]
1100	No bound state	-	-	-	-	-	-
1136	-0.10	3871.10	91.9	0.3	7.5	0.3	7.5
1150	-0.40	3870.80	86.0	0.5	13.0	0.5	4.8
1160	-0.71	3870.49	82.1	0.6	16.7	0.7	3.7
1168	-1.02	3870.18	79.2	0.7	19.3	0.7	3.1
1200	-2.65	3868.55	70.5	1.0	27.5	1.0	1.9
1250	-6.32	3864.88	62.6	1.3	34.9	1.3	1.3
1300	-11.10	3860.10	58.2	1.5	38.8	1.5	1.0
1350	-16.87	3854.33	55.5	1.7	41.1	1.7	0.8

TABLE II: Binding energies with varying  $\Lambda$  in the isospin symmetry limit.

$\Lambda$ [MeV]	$E_{\text{bin}}$ [MeV]	$E = M_0 + E_{\text{bin}}$ [MeV]	$P(0_S)\%$	$P(0_D)\%$	$P(\pm_S)\%$	$P(\pm_D)\%$	rms( $0_S$ ) [fm]
1000	No bound state	-	-	-	-	-	-
1050	-0.06	3871.14	49.7	0.3	49.7	0.3	5.9
1076	-0.41	3870.79	49.5	0.5	49.5	0.5	3.7
1090	-0.71	3870.49	49.4	0.6	49.4	0.6	2.9
1100	-0.97	3870.23	49.3	0.7	49.3	0.7	2.5
1150	-2.94	3868.26	49.1	0.9	49.1	0.9	1.6
1200	-5.95	3865.25	48.9	1.1	48.9	1.1	1.2
1250	-9.98	3861.22	48.7	1.3	48.7	1.3	0.9

TABLE III: Binding energies of the  $BB^*$  system.

Isospin	$J^{\text{PC}}$	$\Lambda$ [MeV]	$E_{\text{bin}}$ [MeV]	$E = M_0 + E_{\text{bin}}$ [MeV]	$P(S)\%$	$P(D)\%$	rms( $S$ ) [fm]
I=0	$1^{++}$	600	-6.32	10598.08	97.90	2.10	1.24
		650	-1.67	10602.73	97.65	2.35	1.91
		700	-0.39	10604.01	97.86	2.14	3.41
		750	-0.33	10604.07	97.72	2.28	3.62
		800	-1.09	10603.31	96.90	3.10	2.15
		850	-3.28	10601.12	96.32	3.68	1.38
		900	-7.33	10597.07	95.97	4.03	1.02
	$1^{+-}$	950	No bound state	-	-	-	-
		1000	-0.34	10604.06	92.70	7.30	3.92
		1050	-2.01	10602.39	86.24	13.76	1.84
		1100	-5.88	10598.52	82.06	17.94	1.20
		1150	-12.72	10591.68	79.45	20.55	0.89
		1200	-23.22	10581.18	77.83	22.18	0.71
		1250	-38.00	10566.40	76.80	23.20	0.59
I=1	$1^{++}$	4700	No bound state	-	-	-	-
		4750	-0.01	10604.39	98.98	1.02	9.01
		4800	-0.06	10604.34	98.40	1.60	7.00
		4850	-0.14	10604.26	97.70	2.30	5.25
		4900	-0.26	10604.14	96.97	3.03	4.03
		4950	-0.41	10603.99	96.24	3.76	3.22
		5000	-0.62	10603.78	95.52	4.48	2.67
	$1^{+-}$	1950	No bound state	-	-	-	-
		2000	-0.04	10604.36	99.45	0.55	7.47
		2050	-0.17	10604.23	99.10	0.90	4.75
		2100	-0.37	10604.03	98.79	1.21	3.28
		2150	-0.67	10603.73	98.53	1.47	2.50
		2200	-1.06	10603.34	98.30	1.70	2.02
		2250	-1.55	10602.85	98.11	1.89	1.70